Improving CSD-Grown REBCO Thin Films by ACAC Addition to the Precursor Solution

Carl Bühler, Manuela Erbe,* Pablo Cayado,* Jens Hänisch, and Bernhard Holzapfel

ABSTRACT: $Gd_{0.5}Y_{0.5}Ba_2Cu_3O_{7-x}$ thin films have been grown from solutions of metal trifluoroacetates dissolved in methanol. These precursor solutions are well suited for chemical solution deposition because of their good wettability and long shelf lives. This could allow for high reproducibility of metalorganic decomposition and film growth if not counteracted by the highly hygroscopic nature of the solutions. Exposure to moist air can result in significant absorption of water with detrimental effects on microstructural film integrity, making the solutions and as-deposited films difficult to handle. To overcome this issue, acetylacetone (acac) has been introduced to the solutions as an additive. The complexing nature of this agent leads to strong interactions with the salts of Cu and the rare earth elements,

reducing the sensitivity to humidity significantly. Films grown from acac-containing solutions are considerably smoother and denser, which in turn leads to enhanced current-carrying capabilities. To investigate the role of acac and its impact on the microstructure and superconducting properties of the films, infrared spectroscopy and thermogravimetry coupled with differential thermal analysis have been performed on different types of solutions and films with and without acac. The microstructural features of the films have been thoroughly compared by scanning electron microscopy. The superconducting properties, T_c and J_c, have been measured by inductive and resistive techniques. Particular focus has been put on the film characteristics that develop with varying amounts of moisture in the process gas during the decomposition of the metalorganic compounds.

1. INTRODUCTION

Chemical solution deposition (CSD)[1] of trifluoroacetates (TFAs) is an established, cost-efficient, and easy-to-scale way to prepare biaxially textured superconducting $REBa_2Cu_3O_{7-x}$ (REBCO, RE = rare earth) films.[2,3] This process generally comprises the following steps. First, a coating solution containing the trifluoroacetate salts of the required REBCO metal cations is prepared and deposited onto a substrate. Subsequently, the resulting precursor film is pyrolyzed to decompose the TFA compounds into a mostly amorphous oxyfluoride matrix. Finally, REBCO is formed from this matrix in a crystallization step.

A major obstacle to achieving reproducible film properties is the hygroscopic nature of the coating solutions and as-deposited precursor films,[4] which is explained by the high Lewis acidity of the TFA salts.[5,6] H_2O−TFA bonds are stronger than methanol−TFA bonds, causing water absorption, which is further increased by the hydrophilicity of the solvent itself. This characteristic, in combination with big differences in vapor pressure (3.17 kPa for H_2O vs 16.3 kPa for methanol) and surface tension (72.9 mN/m for H_2O vs 22.5 mN/m for methanol, at 20 °C) between water and methanol, distorts the precursor species aggregation, which leads to stress states in
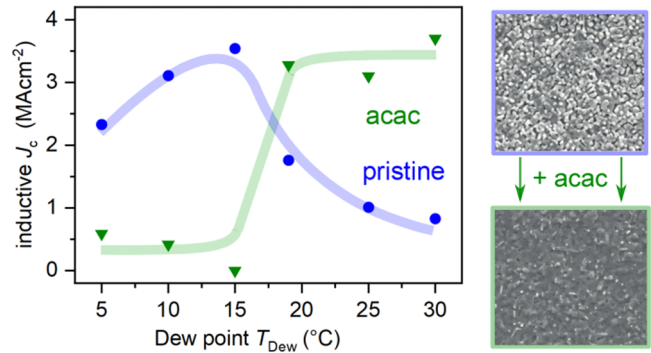
the film. This stress is likely to cause instabilities in the layer, leading to buckling or even cracks.[4] If exposed to high degrees of air moisture, the films require significantly longer pyrolysis times compared to purified solutions.[7] Alternatively, an elaborate purification process of the coating solutions can be applied to remove water and other impurities.[8] This approach also requires extensive precautionary measures to prevent exposure of the refined solutions and as-deposited films to humidity.[4,7] Yet, humidity is also needed later in pyrolysis to avoid sublimation of volatile Cu-TFA[2,4,9] and to increase film elasticity, which prevents the formation of stress-induced defects from film shrinkage.[4] To balance the positive and negative effects of humidity during pyrolysis, the introduction of water to the process gas must be controlled carefully. Another and more promising way to cope with those water-

related drawbacks is the modification of pristine solutions with additives. In a topical review by Obradors et al.,[3] the effectiveness of additives as thermal stabilizers has been examined. Thermally stabilized precursor solutions can positively influence the decomposition of the salts and thereby shorten pyrolysis times while simultaneously improving structural relaxation and plastic flow of the films. Particularly, polydentate ligands such as diethanolamine[10] and other O- and N-donor-ligands, e.g., tetrahydrofuran or N,N,N',N'',N''-pentamethyldiethyletriamine[6] help to stabilize the solutions against the ingress of ambient water. Erbe et al.[9] suggested 2,4-pentanedione, also known as acetylacetone ("acac"), as an effective additive to REBCO coating solutions, reducing the susceptibility to water. This additive has been previously known from sol−gel routes toward thin films of lead zirconate titanate (PZT)[11,12] and $MgTiO_3$.[13] Both materials are interesting candidates for several (micro-)electronic applications, which require dense and homogeneous films with optimal electrical properties. Therefore, acac had been introduced as a chelating agent for the titanium alkoxide salts, making them less prone to hydrolysis, which in turn results in denser films with improved electrical properties.

The present work analyses the interactions between acetylacetone, the REBCO precursor materials, and moisture during pyrolysis by comparing the superconducting and morphological properties of $Y_{0.5}Gd_{0.5}Ba_2Cu_3O_{7-x}$ (YGdBCO) films fabricated from pristine and acac-modified solutions under various pyrolysis conditions. For this, the amount of humidity and the time of its introduction to the pyrolysis gas are varied. The thermal decomposition of the pristine precursors is analyzed by thermogravimetry and differential thermal analysis (TG-DTA) and compared to the data of acac-modified precursors. Deposited films are quenched from different steps of the pyrolysis in dry and humid conditions and analyzed with infrared spectroscopy to understand the role of acac during the pyrolysis. It could be demonstrated that the addition of acetylacetone to the coating solution greatly decreases its susceptibility to ambient humidity. This allows for more humid pyrolysis atmospheres, which results in higher homogeneities of the superconducting films.

2. EXPERIMENTAL SECTION

2.1. Sample Preparation.
The coating solutions were fabricated following the guidelines of Araki et al.[2] Stoichiometric amounts of Gd-, Y-, Ba-, and Cu-acetates with a molar ratio of 1:1:4:6 were mixed with ultrapure water. The resulting heterogeneous mixture was fully dissolved by adding trifluoroacetic acid (TFAH) in excess, which resulted in a pale blue solution. Removal of the solvent by vacuum evaporation at 48 °C down to 5 hPa led to a blue residue mainly consisting of the TFA salts. To eliminate the remaining traces of water and free acid, the gel-like residue was diluted in anhydrous methanol and dried in a rotary evaporator. This process was repeated two times. The result was a brittle, dark blue solid that was dissolved in anhydrous methanol to form a blue 0.25 RE-molar coating solution. These steps were carried out with extensive care to prevent water ingress. For the modified solutions, acac was added to a sample volume of the batch solution, yielding a concentration of vol %, which had been previously determined as the optimum.[9] This corresponds to a molar acac/RE ratio of approximately 0.4 and changes the color of the solution from blue to green. The individual precursor trifluoroacetates were fabricated following the same procedure as for the full coating solutions but with twice the acac concentration, that is 0.8 molar acac/RE ratio, to facilitate qualitative proof of acac in later analysis.

Cleaned and dried 1 cm × 1 cm (100)-oriented $LaAlO_3$ (LAO) single-crystal substrates were spin-coated with these solutions in a dry N_2 atmosphere (dew point < −25 °C) with a constant acceleration over 1 s to 6000 rpm, followed by a 30 s dwell.

The samples were then heat-treated with a thermal profile consisting of three main sections: pyrolysis, crystallization, and oxygenationFigure 1. The ramps marked as (I), (II), and (III)
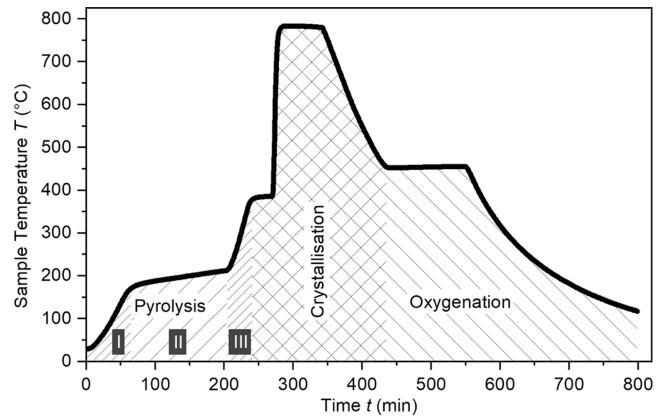
Figure 1. Thermal profile of the heat treatment. During the pyrolysis, important ramps are marked with (I), (II), and (III). The atmospheres are: (I) O_2, 3 cm/s; (II) and (III) O_2, 6 cm/s; crystallization in Ar with 150 ppm O_2, 6 cm/s; oxygenation in O_2, 6 cm/s. Standard heating ramps are (I) 200 K/h, (II) 14 K/h, and (III) 300 K/h, crystallization with a maximum output power of the furnace.

are of special interest here as the humidity conditions during the pyrolysis are varied therein. Depending on the requirements, the samples were either exposed to the full thermal process or quenched at different stages during the pyrolysis..

2.2. Characterization.
The morphology of the films was imaged with a Hirox SH-5000M tungsten scanning electron microscope (SEM). Additional high-resolution images were taken with a Zeiss LEO 1530 FEG-SEM. Critical current densities, J_c, were determined inductively ($J_{c,ind}$) and/or resistively ($J_{c,res}$). For the latter case, 1 mm long microbridges were structured by photolithographic masking and etching in a 0.04 molar HNO_3 solution. The resulting bridge dimensions of ∼50 μm width and typically 220 nm film thickness were determined by a Bruker Dimension Edge atomic force microscope. $J_{c,res}$ was determined in a Quantum Design physical properties measurement system at a 1 μV/cm criterion using a four-probe layout. To minimize resistive heating, the contact areas were coated with a 200 nm gold layer by pulsed laser deposition. $J_{c,ind}$ was determined with a calibrated THEVA Cryoscan in self-field at 77 K at a 50 μV criterion, which was equivalent to the 1 μV/cm criterion of the transport measurement.

The thermal decomposition was analyzed by thermogravimetry (TG) and differential thermal analysis (DTA) on a Netzsch STA 440 in heating up to 400 °C at 2.5 K/min and compared to the data of acac-modified precursors. For this, the solutions were completely dried in a rotary evaporator and ground to a powder to prevent atmospheric deviations due to excessive methanol release in the crucible. Briefly, 30 mg of the
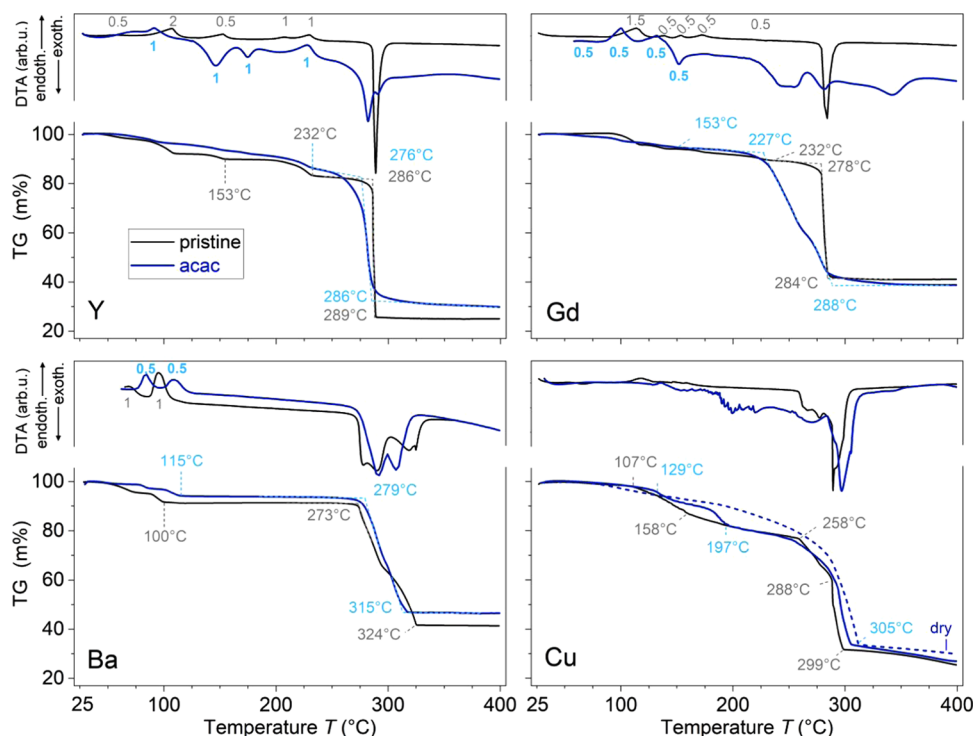
Figure 2. TG-DTA analysis of the TFA (black) and TFA-acac (blue) salts of the four REBCO metal cations Y, Gd, Ba, and Cu. The experiments were run in humid oxygen at a temperature ramp of 2.5 K/min (solid lines). For Cu-TFA-acac, an additional run in dry oxygen (dashed blue line) was performed to separate hydrolysis from other decomposition events. The numbers in the DTA sections refer to the molar amounts of water released from the compound in the corresponding step.

obtained powder was used. For standard humid pyrolysis conditions, the process gas oxygen was passed through a water reservoir with a total gas flow of 70 mL/min. To simulate dry pyrolysis conditions, pure oxygen with a similar flow rate was used as process gas. The beginning and end of a chemical reaction are defined as the intersection between a tangent to the steepest slope of a mass loss and the extrapolated corresponding baseline. The presence of acac-containing compounds in solutions or in films quenched from different steps of the pyrolysis was determined with a Bruker Vertex 70 ATR-IR spectrometer to understand the role of acac during the pyrolysis. The quenched films were placed directly onto the attenuated total reflection (ATR) crystal, whereas for solution measurements, the crystal was continuously flushed with fresh solution to avoid deviations caused by the absorption of humidity.

3. RESULTS AND DISCUSSION

3.1. Thermal Decomposition of Individual Precursors.
For all analyzed precursor materials, except for Cu-TFA, the thermal decomposition is very similar in moist O$_2$, Figure 2, solid lines. An initial, gradual multistep dehydration process, in which coordinated water is removed, is followed by an abrupt exothermic decomposition, in which the final products of the pyrolysis are formed. For Cu-TFA, the gradual mass loss is not attributed to dehydration but to a hydrolysis reaction that releases TFAH from the precursor[14] and is initiated by either coordinated or ambient water from the process gas.

3.1.1. RE-TFA and RE-TFA-ACAC. The thermal decompositions of both the RE-TFA- and the RE-TFA-acac salts of the Y- and Gd-compounds are particularly similar; Figure 2, upper panels. The most important steps are marked by

temperatures within the TG curves, which are displayed in the lower section of the panels. The corresponding DTA signals are plotted above in the upper part of the panels. For the dehydration steps, the molar amounts of water released per mol of metalorganic salt are indicated in the DTA sections by numbers.

Both acac-free Y- and Gd-trifluoroacetates (black thin lines, dark-gray numbers) contain coordinated water, which is removed stepwise in mostly endothermic reactions. Only for the last 0.5 mol of water per 1 mol Gd-TFA, an almost imperceptible upward slope in the DTA signal indicates an exothermic release. In total, Gd-TFA releases 3.5 mol and Y-TFA 5.0 mol water per mol of salt. The presence of acac (blue thick lines and light-blue bold numbers) reduces this amount in both RE salts to 2 (Gd) and 4 (Y) mol per mol of salt, respectively, and changes its release pattern. For Y-TFA-acac, the central two dehydration steps now release energy, while the last dehydration step in the Gd-TFA-acac is now clearly exothermic. Despite the distinct DTA signals, the mass losses proceed more gradually in the acac-containing samples when compared to their acac-free references. In Gd-TFA-acac, the dehydration reaction also ends earlier at 153 °C instead of 232 °C when acac is added. For Y-TFA-acac, no such shift is observed. It is concluded that acac reduces the amount of water coordinated in the respective salts, facilitates its removal as indicated by DTA, and renders the mass loss more gradual during the dehydration stage of the pyrolysis reaction. For Gd-TFA-acac, the facilitation of the water release is also observable through an earlier end of the dehydration reaction. In Y-TFA-acac, the end of the dehydration remains unchanged by the addition of acac at 232 °C. Therefore, the additive appears not to influence the removal of the most strongly bound water in the Y-salt. This last removal of two molecules of water from Y-

TFA in a back-to-back two-step process has neither been reported by Mosidaz et al.[15] nor by Eloussifi et al.[16] and must hence be specific to our solution fabrication procedure. The prior three mol released up to 153 °C, though, correspond both in amount and temperature to the observations by the two research groups.

According to the TG and DTA results, the decomposition of the anhydrous pristine RE-TFA compounds occurs abruptly in exothermic one-step reactions starting at 278 °C (Gd) and 286 °C (Y), respectively. They end at 284 °C (Gd) and 289 °C (Y) and leave the corresponding REF_3 as remains, as confirmed by consistent values of the theoretical and measured mass loss and supported by the literature for the yttrium species.[15] For Y-TFA, the observed decomposition is considerably sharper than reported by other groups, e.g., 275−330 °C in ref 15. Similar to the observations from the dehydration, the acac-modified samples decompose more gradually, forming the same RE-fluorides as their acac-free analogues. For the Y-species, the transition is widened by 7 °C (from 276 to 286 °C) but shows very rounded shapes for both on- and offset of the TG curve as well as two obvious steps according to the DTA signal. We attribute the first signal to an acac-containing species and the second to acac-free Y-TFA. Gd-TFA-acac decomposes in an even more complex manner and wider temperature range from 227 to 288 °C with up to four steps involved. According to the TG signal, there are two steeper sections, whereby the first one shows a prolonged or possibly split exothermic DTA signal pointing to two consecutive decomposition steps. After the third exothermic DTA signal, i.e., after the second steep drop in the TG curve, another step with a very gentle mass decrease takes place, which is clearly supported by a fourth and quite broad exothermic DTA signal. The scale of this very last mass loss of about 4% is smaller than the overall amount of acac added to the salt (about 15 wt %) and significantly smaller than the amount of TFA present (∼48 wt %). The gradual transitions between the slopes without clear steps make calculations difficult, but obviously, more than two species decompose. With an acac/metal ratio of 0.8, more than half of the Gd ions might be involved with acac, forming "mono-", "di-" and "tri-acac" species, which decompose together with Gd-TFA after one another. Presumably, the mono-acac Gd-TFA species forms the largest portion and decomposes in the first steep slope together with a small portion of di-acac complex. The liberated acac may lead to the observed acceleration of the decomposition of the acac-free Gd-TFA species, which is presented by the second steep mass loss. Hereafter, a very small portion of pure "Gd-acac" might explain the last decrease of the mass up to almost 350 °C. In conclusion, acac causes an earlier beginning of the decomposition and retards the full conversion into the REF_3 to 340 °C (Gd) and 330 °C (Y), respectively. Using the example of the Gd-salts, acac allows for a drastically more gradual decomposition from only a few centigrades to more than a hundred. Such a prolonged decomposition behavior is also known from the pure $RE(acac)_3$ species of both Y and Gd.[17,18]

3.1.2. Ba-TFA and BA-TFA-acac. Pristine Ba-TFA dehydrates in a two-stage process that tapers off at 100 °C, Figure 2; bottom left, and releases 2 mol H_2O per mol of salt. This is in accordance with refs 19, 20. Acac-modified Ba-TFA behaves similarly, releasing an equivalent of 1 mol H_2O in two steps finishing at 115 °C. Ba-TFA appears to coordinate water only weakly and in little quantities. It is therefore assumed to play only a minor role in the sensitivity of REBCO precursor films to humidity.

After a long plateau without discernible mass loss, the thermal decomposition of the pristine material begins at 273 °C and ends at 324 °C as a two-stage process, which is similar to results in the literature.[19,20] The remaining mass after the first decomposition step suggests the formation of intermediate $CF_3COOBaF$[19,20] before BaF_2 is ultimately formed. The pyrolysis of the acac-modified salt sets in slightly delayed at 279 °C. It follows a similar two-step process that also ends slightly earlier at 315 °C. However, the two steps cannot be clearly separated in the TG graph, which hinders further analysis of the acac and TFA decomposition. In summary, the differences between modified and pristine material are considerably smaller than for the other species. Thus, acac may not have a substantial effect on the overall thermal decomposition of the Ba salt in REBCO precursor solutions.

3.1.3. Cu-TFA and Cu-TFA-acac. Both Cu-TFA and Cu-TFA-acac contain very small quantities of water of at most 0.5 mol per mol of salt, which is released up to 107 and 129 °C, respectively, Figure 2; bottom right. Subsequent contact of pristine Cu-TFA with humidity during the heat treatment causes hydrolysis of the precursor, resulting in the release of TFAH before further anhydrous decomposition takes place—similar to results reported on commercial Cu-TFA.[14] According to the steps in the TG curve, the mass drops in three major stages, at the end of which CuO is formed. The DTA signal shows several finer split-ups of the signal. Beginning at 107 °C, TFAH is released endothermically, leading to the formation of $Cu_2(CF_3COO)_3OH$. Presumably, this species is responsible for the inhibition of the detrimental Cu-sublimation in TFA-MOD-derived films due to a decreased volatility caused by H-bonds.[2,9,14] This hydrolysis reaction reaches a maximum rate of around 158 °C, after which it tapers off. The second stage of decomposition begins at 258 °C, showing a mass loss at a nearly constant rate up to 288 °C. This reaction is exothermic, which indicates oxidation of parts of the precursor under the release of more TFAH, CO_2, and other decomposition gasses.[14,21] The reaction ends when the intermediate species $Cu(CF_3COO)_2CuO$ has formed.[14] Subsequently, the final formation of CuO starts at 288 °C and ends at 299 °C. It occurs in two exothermic reactions, leading to an abrupt mass loss. An ensuing, slow mass loss is also observed, which is attributed to the removal of remaining carbon from the crucible. The recorded temperature of the main decomposition step at 288 °C is higher than reported by Mosiadz et al. in humid O_2 (209−212 °C)[14] but is in the range observed by Gupta et al.[22]

For acac-modified samples, the hydrolysis proceeds in two steps between 129 and 197 °C. The first part can be attributed to the hydrolysis of 0.2 mol TFA per mol of Cu salt, which presumably proceeds to hydrolysis of another 0.3 mol acac to give $Cu_2(TFA)_2(acac)OH$ at around 180 °C. Hereafter, the rest of the decomposition runs rather parallel to the acac-free species, with a slight delay of the end point (305 °C instead of 299 °C) and a more rounded shape without clear steps in the TG curve. The dashed blue line in Figure 2 shows the course of the TG signal of Cu-TFA-acac in dry oxygen to illustrate the missing hydrolysis steps in the absence of humidity.

3.2. IR Spectroscopy. First, the coating solution and solutions of the individual salts with and without acac are measured by IR spectroscopy (Figure 3). The results are later

compared to thin films (Figure 4) after pyrolysis to understand under which conditions acac is expelled from the sample.
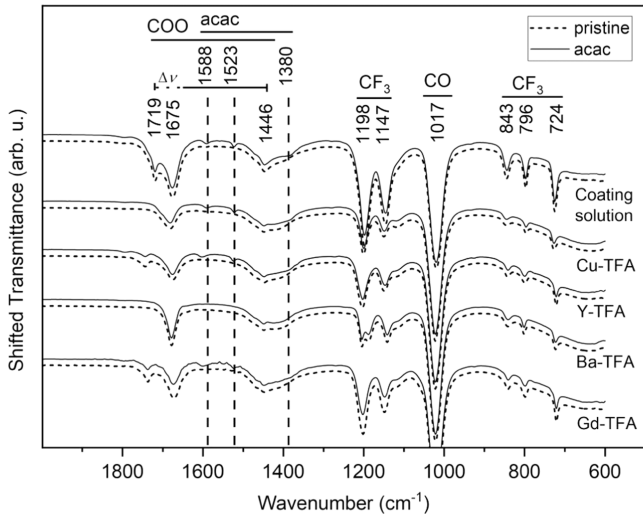
Figure 3. IR spectra of a 0.25 molar methanolic GdYBCO coating solution (top) in comparison to the individual components (below). Solid lines depict samples modified with 0.4 (coating solution) and 0.8 acac/M (M-TFA solutions). Dashed lines represent the pristine solutions.
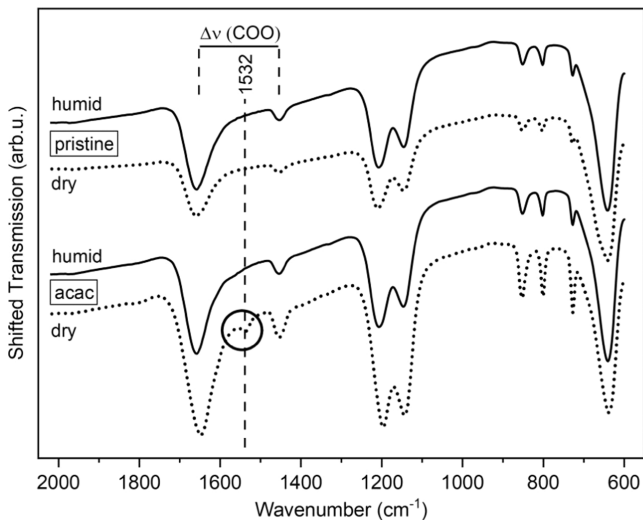
Figure 4. IR Spectra of films quenched from pyrolysis at 280 °C in dry (dotted lines) and humid (solid lines) conditions. The solutions for the films were either pristine or modified with 0.4 acac/RE. $\Delta\nu$ of the carboxylate group is reduced compared to the coating solution. The acac-related absorption band at 1532 cm^{-1} is only visible for samples reacted in a dry atmosphere.

3.2.1. Solutions. In the coating solutions, the band at 1017 cm^{-1} is caused by the C−O vibration of methanol. The bands at 1198 and 1147 cm^{-1} are assigned to vibrations of the CF$_3$ group[23] of TFA. The absorption at 1675 cm^{-1} corresponds to the asymmetric vibration of the carboxylate group,[24] while the band at 1446 cm^{-1} is caused by the corresponding symmetric vibration.[24] Both bands are therefore specific to TFA. The difference between the carboxylate bands $\Delta\nu$ is determined by the type of the formed complex. Analysis of this shift allows discerning monodentate complexes, which show increased $\Delta\nu$ values compared to the free anion, from chelates or bridging

ligands, which are expected to show smaller $\Delta\nu$ values.[24,25] The distance between the symmetrical and the asymmetrical vibration amounts to 229 cm^{-1}, which indicates that most TFA is free in the solutions and not specifically bound to a metal cation.[24] The additional peak at 1719 cm^{-1} is caused by a fraction of TFA that forms a monodentate complex. This is a specific property of the trivalent cations of Y and Gd, as can be seen from the IR spectra of the individual compounds.

In the modified coating solution, two additional acac-specific absorption bands appear at 1588 cm^{-1} (asymmetrical C−C stretch) and 1523 cm^{-1} (either symmetrical C−C or asymmetrical C−O stretch).[26] A broader peak occurs around 1380 cm^{-1}, which is attributed to the deformation of the CH$_3$ group of acac.[26] The same peaks with slight deviations can be seen in the individual Y-, Gd-, and Cu-precursors, indicating that these trifluoroacetates form acac-containing compounds in solutions. Two days after mixing, no reaction between acac and the Ba-TFA solution could be measured, even though TG-DTA analysis of the dried solution showed a visible impact of acac on Ba-TFA decomposition. The best conformity of peak positions with the coating solution is achieved in the case of Cu-TFA. The most prevalent acac-containing compound in the coating solution, therefore, appears to be copper-based, as suggested by Erbe et al.[9] This also reflects the experience of preparing acac-modified solutions. Addition of acac to methanolic Cu-TFA solutions instantly turns the solution from blue to green, whereas Gd- and Y-TFA solutions take several minutes to change color. No color change was observed for the modified Ba-TFA solutions.

3.2.2. Films. Figure 4 shows the typical bands in the IR spectra that are expected for films quenched from the pyrolysis at 280 °C with either dry or humid conditions. The C−O vibration of methanol at 1017 cm^{-1} has vanished due to the evaporation of the solvent. The absorption band caused by monodentate Gd- and Y-TFA complexes at 1719 cm^{-1} is also not observed anymore, while $\Delta\nu$ is reduced to 194 cm^{-1}. Both observations indicate that the acid residual anions form chelate or bridging complexes with the metal cations in the film.

In the dry, acac-modified sample, the acac-related absorption at 1588 cm^{-1} is covered by the shifted band of the carboxylate group, but the C−C/C−O vibration at 1532 cm^{-1} is still well visible. This band is not visible in samples pyrolyzed in humid conditions, indicating that acac is mostly removed from the precursors below 280 °C if humidity is introduced to the pyrolysis gas. Under the assumption that acac preferentially reacts with Cu-TFA, this confirms previous observations that acac bound to Cu-TFA decomposes at least partly in a hydrolysis reaction at low temperatures and the rest, most likely, in the early main decomposition stage when the hydroxy species Cu$_2$(TFA)$_2$(acac)OH forms Cu(TFA)$_2$CuO. It also supports the assumption that the acac species decompose before acac-free Y-TFA in the acac-modified Y-TFA solution and that large parts of acac in the Gd compound are removed before Gd-TFA as well.

3.3. Influence of Humidity and ACAC on the Superconducting and Morphological Film Properties. Figure 5 compares the dependence of J_c of fully processed pristine and acac-modified films on the time at which humidity was added to the initially dry process gas during pyrolysis. The temperature−time profile of the pyrolysis (black curve) was the same for all samples, and a dew point of 19 °C was adjusted as soon as the humidity was introduced.
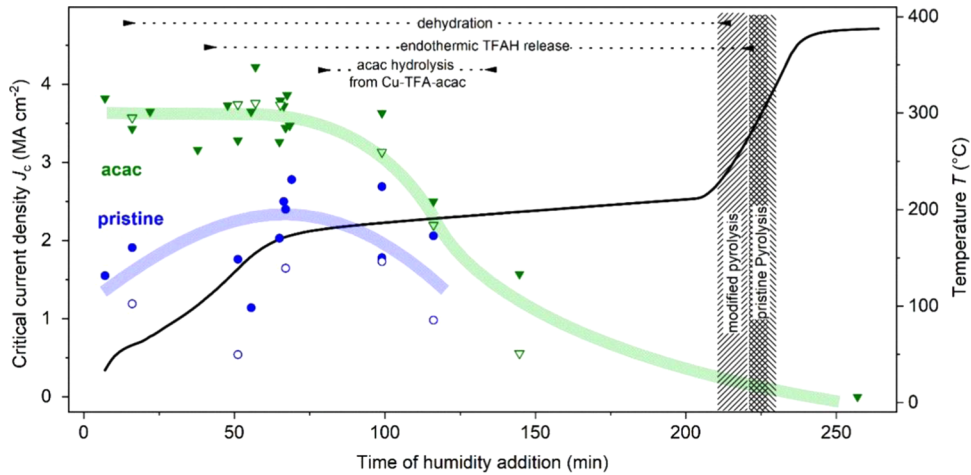
Figure 5. Primary axis: inductive (closed symbols) and resistive (open symbols) J_c values of acac-modified (green triangles) and pristine (blue circles) films over their respective time of dew point adjustment. Secondary axis: pyrolysis profile (black curve) and areas of exothermic decomposition determined for pristine samples and samples modified with 0.4 acac/RE. Shaded lines are guides to the eyes.
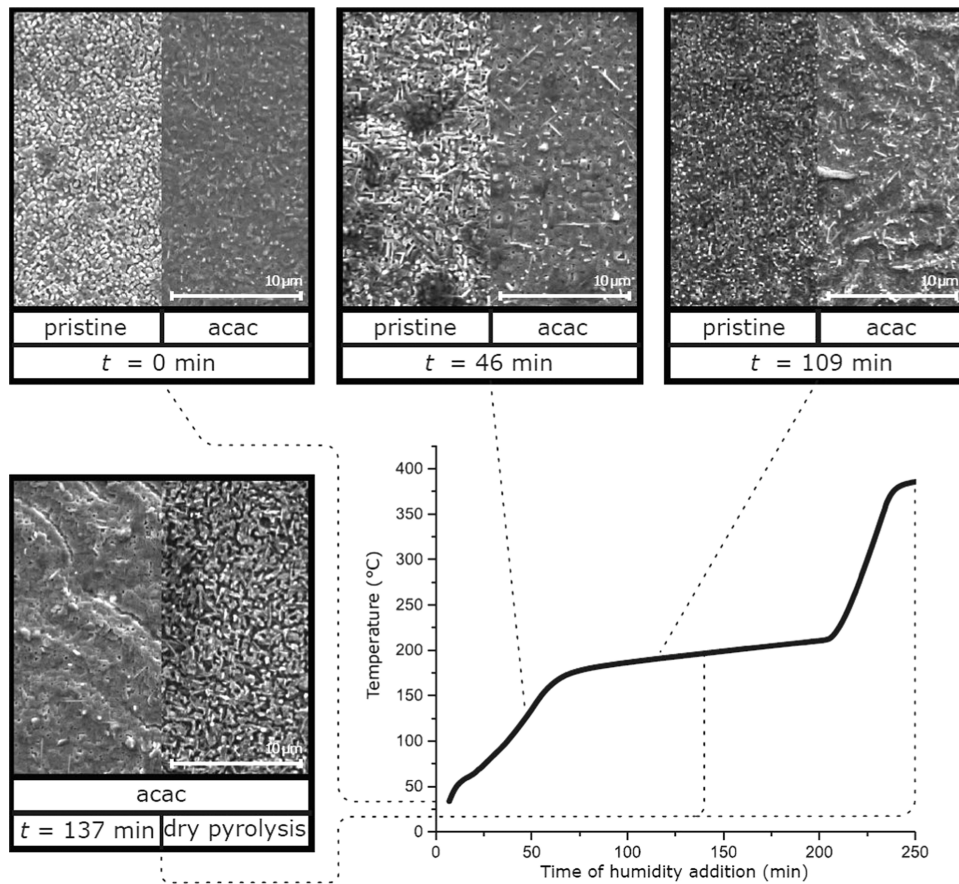
Figure 6. Film surface morphologies after crystallization depending on the time t of humidity addition to the pyrolysis atmosphere; black curve: $T-t$ profile of pyrolysis.

The addition of acac (green triangles) distinctly increases both the overall inductive (closed symbols) and resistive (open symbols) critical current densities. The maximum inductive values recorded are 2.8 MA/cm^2 for the pristine samples (blue circles) and 4.2 MA/cm^2 for the acac-modified ones. This is a total improvement of 52% in $J_{c,ind}$. The critical current density for pristine samples is severely reduced if humidity is introduced too early (i.e., before 70 min). This confirms earlier reports[2,4,7] stating that un-pyrolyzed, TFA-MOD-

derived precursor films are damaged by the absorption of humidity. Contrarily, the acac-modified samples do not degrade when moisture is added early on and deliver more reproducible critical current densities. Both aspects demonstrate that acac-modified films are significantly more stable in humid atmospheres.

Unlike inductive measurements, transport measurements are highly sensitive to defects that narrow the superconducting cross section such as ab-grains, voids, and surface roughness. A

disparity between the inductive and the resistive measurement, therefore, indicates inhomogeneous morphologies. Prior to the 100 min mark, these deviations are significant only in pristine samples and vanish in acac-modified samples. This is a clear indication that films from acac-modified solutions crystallize denser and more homogeneously.

If humidity is added after 100 min, the critical current density gradually decreases for acac-modified and pristine films alike. This is believed to be partially caused by copper sublimation.[4] Without water in the pyrolysis gas, the formation of the less volatile intermediate $Cu_2(CF_3COO)_3(OH)$ is impaired,[2,14] which leads to an aggravated sublimation of Cu-TFA and finally to an off-stoichiometric composition with reduced critical current densities.[2] A delayed water addition also results in an increased difference between the inductive and resistive J_c values, which indicates an increasingly disturbed morphology as, e.g., caused by stress-induced defects such as cracks and buckling, or porosity from gaseous species such as sublimating Cu-TFA or decomposition gases.

Figure 6 depicts the development of the film morphologies for different times of humidity addition for acac-modified and pristine films. Late addition, after 100 min, always leads to visible cracks and severe buckling, regardless of whether the film contains acac or not. This is in accordance with the simultaneous decrease of J_c and indicates that humidity is generally required for a defect-free morphology of the final film. Clearly, acac also allows an early introduction of water during pyrolysis—even from the beginning—whereas pristine films show an increasing granularity in that case. Generally, the morphology of acac-modified films presents itself considerably more dense and homogeneous in the entire range of humidity addition. After completely dry pyrolysis, though, the acac-modified film is also massively shattered, which is probably caused by a loss of film plasticity and therefore a lack of ability to cope with a sudden release of gaseous decomposition products. These structural inhomogeneities in acac-modified films, which intensify with humidity onset times beyond the 100 min mark, can be directly correlated with delayed or absent hydrolysis of the Cu-TFA-acac species, see Figure 5.

Besides the time of humidity addition, the film quality also depends on the amount of water in the process gas, as can be seen in Figure 7. Therefore, the dew point was varied between 5 and 30 °C for both pristine and acac-modified samples. To prevent damage to the pristine films due to a premature humidity exposure, the time of humidity addition was set to 50
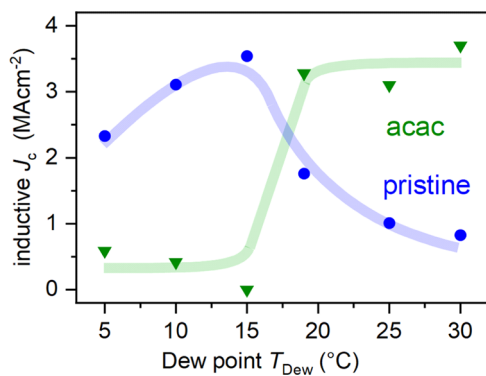
min in this case, which corresponds to 134 °C and matches the optimized range of the J_c–t correlation of Figure 5. The pristine samples exhibit a maximum inductive critical current density of 3.5 MA/cm^2 at a dew point of 15 °C (Figure 7). Toward higher dew points, J_c gradually decreases down to 0.83 MA/cm^2 at 30 °C. This is in accordance with the observation that pristine precursor films can undergo damage from exposure to humidity. As some water is required to inhibit copper sublimation and enhance the plasticity of the film, dew points lower than 15 °C result in a similar decay of J_c. Contrarily, the acac-modified films show very low J_c values for dew points up to 15 °C and an abrupt increase to ∼3.5 MA/cm^2 between 19 and 30 °C. Based on the TG-DTA and IR data, it seems most likely that the hydrolysis and thereby removal of parts of acac before the pyrolysis are a necessity to fabricate high-J_c films from acac-modified solutions. Dry pyrolysis circumvents the formation of $Cu_2(TFA)_2(acac)OH$ and leads to the simultaneous decomposition of all acac and TFA components, which is detrimental to the film properties. The pivotal influence of humidity was crosschecked by varying the time that a sample was exposed to humidity by changing the length of ramp II. The results were identical. In both scenarios, acac led to films that tolerated significantly more humidity.
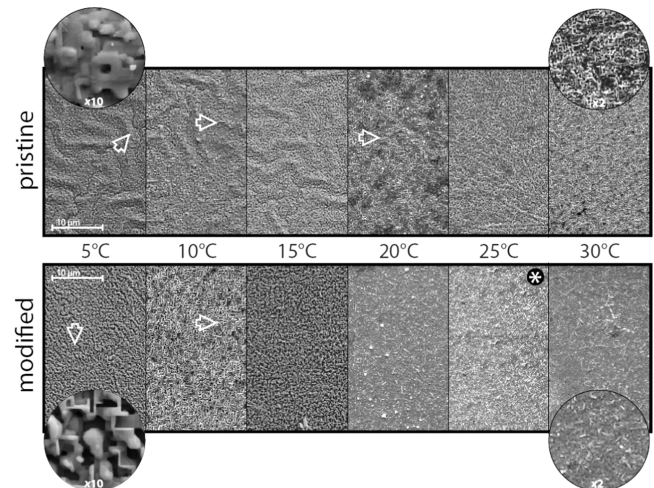
Figure 8. Influence of the dew point during the pyrolysis on the surface morphology of films grown from pristine (top) and acac-modified (bottom) solutions. Hill-shaped areas represent buckling, and cracks can be seen as black trenches. In circles: corresponding 10✕- or 2✕- enlargements of the respective images. All samples are fabricated by introducing humidity at 134 °C.

The SEM images in Figure 8 compare the influence of the dew point on the surface morphology of pristine and acac-modified films. Below a dew point of 15 °C, pristine films have denser morphologies, as there is little damage due to the absorption of humidity. These films are buckled and cracked though, which is caused by the reduced pliability of the films in dry conditions and the ensuing high stresses during shrinkage.[4] The film grown with the least humidity is composed of thin, overlapping rectangular plates (see enlargement). With increasing amount of humidity, the microstructure appears more nodular and finally maze-like. In the final, severely damaged state of 30° dew point, the plates form a porous, needle-like network. The small junctions between such needles

Figure 7. Dew point dependence of the critical current density of GdYBCO thin films grown from acac-modified (green triangles) and pristine (blue circles) solutions.

result in locally increased current densities, which detrimentally influence the critical current density of the bulk material.

Conversely, acac-modified films are extremely porous when pyrolyzed in dry conditions. This is due to the delayed or inhibited hydrolysis of the acac-containing compound in dry atmospheres as demonstrated by TG-DTA and IR spectroscopy. Without first removing parts of acac and forming the hydroxy species, all acac-containing compounds decompose along with the pristine material in a very narrow temperature range, which leads to disturbed morphologies and eventually reduced J_c values. If the dew point is increased, the film surfaces are first more nodular and then, at a dew point of 20 °C, which seems to suffice for the acac hydrolysis, dense and smooth. Films pyrolyzed from modified solutions in highly humid atmospheres neither buckle nor crack and show less overall porosity compared to the pristine films from dry conditions. The formation of $Cu_2(TFA)_2(acac)OH$ is crucial to the films' stability in humid environments, which allows drastically more humid pyrolysis routes.

4. CONCLUSIONS

The impact of 2,4-pentanedione (acac) as an additive to TFA-MOD coating solutions was analyzed by TG-DTA, IR spectroscopy, SEM, and J_c measurements. The thermal decomposition of pristine Gd-, Y-, Ba-, and Cu-TFA was compared to precursors modified with 0.8 mol acac per contained mol of the metal ion. For Ba-TFA, no significant change in the decomposition through acac could be observed apart from a slight reduction in the amount of water within the crystal structure from 2 to 1, which is loosely bound and thus released at low temperatures. Y- and Gd-TFA showed very similar features of decomposition of the pristine salts and analogue changes toward acac addition. Both pristine salts contain large amounts of water, which is released in several dehydration steps up to the sudden pyrolysis of the metalorganic components. This amount of water is considerably reduced in both salts if acac is added. In Y-TFA derived via the TFA-MOD process, a previously unobserved dehydration step of two further molecules of water per precursor molecule was discovered at high temperatures. In Cu-TFA, hydrolysis of parts of acac takes place before the actual pyrolysis and presumably leads to the formation of the intermediary $Cu_2(TFA)_2(acac)OH$, a species that may play an important role in the development of a smooth microstructure in REBCO films. In summary, for all salts, the addition of acac leads to lower amounts of coordinated water (a total reduction of 33% in an acac-modified REBCO precursor solution), to more gradual transitions between decomposition steps, and to a less abrupt main pyrolysis. In sum, all of this could help to reduce shrinkage-induced defects such as cracks and/or buckling. IR spectroscopy confirmed that early removal of large parts of acac requires humidity.

Pristine films at their dryer optimum were dense but buckled and cracked and could not be hydrolyzed at high dew points. The acac-modified films performed much better regarding their superconducting properties and were more reproducible and less sensitive to humidity. Especially the detrimental influence of humidity at low temperatures could be mitigated completely. This allows for reducing or even omitting complicated and expensive measures of humidity control in the coating process, which greatly facilitates lab-scale and industrial fabrication of TFA-MOD-derived films. Additionally,

acac-modified films showed dense, smooth, and crack-free morphologies if pyrolyzed in humid atmospheres.

AUTHOR INFORMATION

Corresponding Authors
Manuela Erbe − *Karlsruhe Institute of Technology (KIT), Institute for Technical Physics (ITEP), 76344 Eggenstein-Leopoldshafen, Germany*; Email: manuela.erbe@kit.edu

Pablo Cayado − *Karlsruhe Institute of Technology (KIT), Institute for Technical Physics (ITEP), 76344 Eggenstein-Leopoldshafen, Germany; Department of Quantum Matter Physics, University of Geneva, 1211 Geneva, Switzerland;* orcid.org/0000-0003-3703-6122; Email: Pablo.cayado@unige.ch

Authors
Carl Bühler − *Karlsruhe Institute of Technology (KIT), Institute for Technical Physics (ITEP), 76344 Eggenstein-Leopoldshafen, Germany*

Jens Hänisch − *Karlsruhe Institute of Technology (KIT), Institute for Technical Physics (ITEP), 76344 Eggenstein-Leopoldshafen, Germany*

Bernhard Holzapfel − *Karlsruhe Institute of Technology (KIT), Institute for Technical Physics (ITEP), 76344 Eggenstein-Leopoldshafen, Germany*

REFERENCES

(1) Bäcker, M.; Baumann, A.; Brunkahl, O.; Erbe, M.; Schneller, T. Chemical Solution Deposition (CSD). In *Digital Encyclopedia of Applied Physics*; American Cancer Society, 2019; pp 1−34.

(2) Araki, T.; Hirabayashi, I. Review of a Chemical Approach to $YBa_2Cu_3O_{7-x}$-Coated Superconductors—Metalorganic Deposition Using Trifluoroacetates. *Supercond. Sci. Technol.* **2003**, *16*, R71−R94.

(3) Obradors, X.; Puig, T.; Ricart, S.; Coll, M.; Gazquez, J.; Palau, A.; Granados, X. Growth, Nanostructure and Vortex Pinning in Superconducting $YBa_2Cu_3O_7$ Thin Films Based on Trifluoroacetate Solutions. *Supercond. Sci. Technol.* **2012**, *25*, No. 123001.

(4) Jin, L. H.; Zhang, Y.; Yu, Z. M.; Yan, G.; Li, C. S.; Lu, Y. F. Effect of Relative Humidity on Morphology of YBCO Films Prepared by CSD Method. *Phys. C* **2010**, *470*, 1257−1260.

(5) Zhang, J.; Morlens, S.; Hubert-Pfalzgraf, L. G.; Luneau, D. Synthesis, Characterization and Molecular Structures of Yttrium Trifluoroacetate Complexes with O- and N-Donors: Complexation vs. Hydrolysis. *Eur. J. Inorg. Chem.* **2005**, *2005*, 3928−3935.

(6) Zhang, J.; Hubert-Pfalzgraf, L. G.; Luneau, D. Synthesis, Characterization and Molecular Structures of Cu(II) and Ba(II) Fluorinated Carboxylate Complexes. *Polyhedron* **2005**, *24*, 1185−1195.

(7) Zalamova, K.; Romà, N.; Pomar, A.; Morlens, S.; Puig, T.; Gázquez, J.; Carrillo, A. E.; Sandiumenge, F.; Ricart, S.; Mestres, N.; Obradors, X. Smooth Stress Relief of Trifluoroacetate Metal-Organic Solutions for $YBa_2Cu_3O_7$ Film Growth. *Chem. Mater.* **2006**, *18*, 5897−5906.

(8) Araki, T. Purified Coating Solution and Growth Scheme of the $YBa_2Cu_3O_{7-x}$ Superconductors in Metal Organic Deposition Using Trifluoroacetates. *Bull. Chem. Soc. Jpn.* **2004**, *77*, 1051−1061.

(9) Erbe, M.; Hänisch, J.; Freudenberg, T.; Kirchner, A.; Mönch, I.; Kaskel, S.; Schultz, L.; Holzapfel, B. Improved $REBa_2Cu_3O_{7-x}$ (RE = Y, Gd) Structure and Superconducting Properties by Addition of Acetylacetone in TFA-MOD Precursor Solutions. *J. Mater. Chem. A* **2014**, *2*, 4932−4944.

(10) Dawley, J. T.; Clem, P. G.; Boyle, T. J.; Ottley, L. M.; Overmyer, D. L.; Siegal, M. P. Rapid Processing Method for Solution Deposited $YBa_2Cu_3O_{7-\delta}$ Thin Films. *Phys. C* **2004**, *402*, 143−151.

(11) Weng, L.; Bao, X.; Sagoe-Crentsil, K. Effect of Acetylacetone on the Preparation of PZT Materials in Sol−Gel Processing. *Mater. Sci. Eng.: B* **2002**, *96*, 307−312.

(12) Schwartz, R. W.; Assink, R. A.; Dimos, D.; Sinclair, M. B.; Boyle, T. J.; Buchheit, C. D. Effects of Acetylacetone Additions on PZT Thin Film Processing. *MRS Proc.* **1994**, *361*, 377−387.

(13) Surendran, K. P.; Wu, A.; Vilarinho, P. M.; Ferreira, V. M. Sol−Gel Synthesis of Low-Loss $MgTiO_3$ Thin Films by a Non-Methoxyethanol Route. *Chem. Mater.* **2008**, *20*, 4260−4267.

(14) Mosiadz, M.; Juda, K. L.; Hopkins, S. C.; Soloducho, J.; Glowacki, B. A. An In-Depth in Situ IR Study of the Thermal Decomposition of Copper Trifluoroacetate Hydrate. *J. Fluorine Chem.* **2012**, *135*, 59−67.

(15) Mosiadz, M.; Juda, K. L.; Hopkins, S. C.; Soloducho, J.; Glowacki, B. A. An In-Depth in Situ IR Study of the Thermal Decomposition of Yttrium Trifluoroacetate Hydrate. *J. Therm. Anal. Calorim.* **2012**, *107*, 681−691.

(16) Eloussifi, H.; Farjas, J.; Roura, P.; Ricart, S.; Puig, T.; Obradors, X.; Dammak, M. Thermoanalytical Study of the Decomposition of Yttrium Trifluoroacetate Thin Films. *Thin Solid Films* **2013**, *545*, 200−204.

(17) Alarcón-Flores, G.; Aguilar-Frutis, M.; García-Hipolito, M.; Guzmán-Mendoza, J.; Canseco, M. A.; Falcony, C. Optical and Structural Characteristics of Y_2O_3 Thin Films Synthesized from Yttrium Acetylacetonate. *J. Mater. Sci.* **2008**, *43*, 3582−3588.

(18) Halmenschlager, C. M.; Neagu, R.; Rose, L.; Malfatti, C. F.; Bergmann, C. P. Influence of the Process Parameters on the Spray Pyrolysis Technique, on the Synthesis of Gadolinium Doped-Ceria Thin Film. *Mater. Res. Bull.* **2013**, *48*, 207−213.

(19) Mosiadz, M.; Juda, K. L.; Hopkins, S. C.; Soloducho, J.; Glowacki, B. A. An In-Depth in Situ IR Study of the Thermal Decomposition of Barium Trifluoroacetate Hydrate. *Thermochim. Acta* **2011**, *513*, 33−37.

(20) Farjas, J.; Camps, J.; Roura, P.; Ricart, S.; Puig, T.; Obradors, X. The Thermal Decomposition of Barium Trifluoroacetate. *Thermochim. Acta* **2012**, *544*, 77−83.

(21) Llordés, A.; Zalamova, K.; Ricart, S.; Palau, A.; Pomar, A.; Puig, T.; Hardy, A.; Van Bael, M. K.; Obradors, X. Evolution of Metal-Trifluoroacetate Precursors in the Thermal Decomposition toward High-Performance $YBa_2Cu_3O_7$ Superconducting Films. *Chem. Mater.* **2010**, *22*, 1686−1694.

(22) Gupta, A.; Jagannathan, R.; Cooper, E. I.; Giess, E. A.; Landman, J. I.; Hussey, B. W. Superconducting Oxide Films with High Transition Temperature Prepared from Metal Trifluoroacetate Precursors. *Appl. Phys. Lett.* **1988**, *52*, 2077−2079.

(23) Redington, R. L.; Lin, K. C. Infrared Spectra of Trifluoroacetic Acid and Trifluoroacetic Anhydride. *Spectrochim. Acta, Part A* **1971**, *27*, 2445−2460.

(24) Deacon, G. B.; Phillips, R. J. Relationships between the Carbon-Oxygen Stretching Frequencies of Carboxylato Complexes and the Type of Carboxylate Coordination. *Coord. Chem. Rev.* **1980**, *33*, 227−250.

(25) Sutton, C. C. R.; da Silva, G.; Franks, G. V. Modeling the IR Spectra of Aqueous Metal Carboxylate Complexes: Correlation between Bonding Geometry and Stretching Mode Wavenumber Shifts. *Chem. - Eur. J.* **2015**, *21*, 6801−6805.

(26) Nakamoto, K.; Martell, A. E. Infrared Spectra of Metal-Chelate Compounds. I. A Normal Coordinate Treatment on Bis-(Acetylacetonato)-Cu(II). *J. Chem. Phys.* **1960**, *32*, 588−597.